

1 **[Technical note] 3-hourly temporal downscaling of monthly global**
2 **terrestrial biosphere model net ecosystem exchange**

3

4 Joshua B. Fisher^{1,*}, Munish Sikka¹, Deborah N. Huntzinger², Christopher
5 Schwalm³, Junjie Liu¹

6

7 ¹ Jet Propulsion Laboratory, California Institute of Technology, 4800 Oak Grove Drive, Pasadena, CA, 91109, USA

8 ² School of Earth Sciences and Environmental Sustainability, Northern Arizona University, 527 S. Beaver St.,
9 Flagstaff, AZ, 86011-5694, USA

10 ³ Woods Hole Research Center, Falmouth, MA, 02540, USA

11 * *Corresponding author. E-mail: jbfisher@jpl.nasa.gov*

12

13 Author contributions: JBF, DNH, and CS formulated idea; JBF and MS designed research; MS performed research;
14 DNH and CS provided data; all authors contributed to the writing of the paper.

15

16 The authors declare no conflict of interest.

17

18 Running title: 3-hourly temporal downscaling of monthly NEE

19 **Abstract**

20 The land surface provides a boundary condition to atmospheric forward and flux inversion
21 models. These models require prior estimates of CO₂ fluxes at relatively high temporal
22 resolutions (e.g., 3-hourly) because of the high frequency of atmospheric mixing and wind
23 heterogeneity. However, land surface model CO₂ fluxes are often provided at monthly time steps,
24 typically because the land surface modeling community focuses more on time steps associated
25 with plant phenology (e.g., seasonal) than on sub-daily phenomena. Here, we describe a new
26 dataset created from 15 global land surface models and 4 ensemble products in the Multi-scale
27 Synthesis and Terrestrial Model Intercomparison Project (MsTMIP), temporally downscaled
28 from monthly to 3-hourly output. We provide 3-hourly output for each individual model over 7
29 years (2004-2010), as well as an ensemble mean, a weighted ensemble mean, and the multi-
30 model standard deviation. Output is provided in three different spatial resolutions for user
31 preferences: 0.5° x 0.5°, 2.0° x 2.5°, and 4.0° x 5.0° (latitude/longitude). These data are publicly
32 available from: ftp://daac.ornl.gov/data/cms/CMS_NEE_CO2_Fluxes_TBMO/data.

33
34 *Keywords: CO₂ flux; downscale; land surface; NEE; sub-daily; hourly*

35 This technical note describes the methodological approach employed with temporally
 36 downscaling monthly terrestrial biosphere model (TBM) net ecosystem exchange (*NEE*) (i.e., net
 37 CO₂ flux between the land and atmosphere) output to 3-hourly time steps (Fisher et al., 2014).
 38 These data were created initially for NASA's Carbon Monitoring System (CMS), and are useful
 39 to the broader land surface and atmospheric scientific community (Fisher et al., 2011; Fisher et
 40 al., 2012). The general downscaling approach follows Olsen and Randerson (2004) with
 41 modifications. The logic takes the components of *NEE*, i.e., gross primary production (*GPP*) and
 42 ecosystem respiration (*Re*), and links them with incident shortwave solar radiation (*I*) and near
 43 surface (2 m) air temperature (*T_a*), respectively. *I* and *T_a* are provided at 6-hourly time steps from
 44 CRU-NCEP (Wei et al., 2014a; Wei et al., 2014b), which we interpolated to 3-hourly time steps
 45 following cosines of solar zenith angle for *I* and linear interpolation for *T_a*. Hence, *GPP* and *Re*
 46 are temporally downscaled to 3-hourly, and re-combined to form *NEE* at 3-hourly time steps.

47
 48 The 6-hourly to two 3-hourly time steps from the solar zenith angle cosine interpolation follows
 49 this equation:

$$I_{t1} = \frac{I_t \times \cos z_{t1}}{\left(\frac{\cos z_{t1} + \cos z_{t-t1}}{2}\right)}, I_{t-t1} = \frac{I_t \times \cos z_{t-t1}}{\left(\frac{\cos z_{t1} + \cos z_{t-t1}}{2}\right)} \quad (1)$$

50 where *z* is solar zenith angle and *I_t* is in units of W m⁻². As an example, if the 0-6 hour *I_t* was 100
 51 W m⁻², and the 0-3 hour *z_{t1}* was 0 (i.e., cos(*z_{t1}*) = 1) and the 4-6 hour *z_{t-t1}* was 60 (i.e., cos(*z_{t-t1}*) =
 52 0.5), then the 0-3 hour *I_{t1}* would be 133.3 W m⁻², and the 4-6 hour *I_{t-t1}* would be 66.7 W m⁻².

53
 54 To scale *GPP* and *Re* to 3-hourly time steps, we followed Olsen and Randerson (2004) with
 55 modifications starting first with the calculation of scale factors based on *I* and *T_a*:

$$Q10_{3hr} = 1.5^{\frac{T_{a,3hr}-30}{10}} \quad (2a)$$

$$T_{scale} = Q10_{3hr} / \sum_{30day} Q10_{3hr} \quad (2b)$$

$$I_{scale} = I_{3hr} / \sum_{30day} I_{3hr} \quad (3)$$

56 where *Q10* is the temperature dependency of *Re*, and *T_a* is in degrees Celsius (converted from
 57 Kelvin, as provided by CRU-NCEP). Note that Olsen and Randerson (2004) originally used time
 58 integral periods of calendar months, but we observed that this caused unrealistic distinct shifts
 59 between months. Instead, we modified the integral period to a 30-day moving window (Figure 1).
 60 For the first 15 days of January of the record and the last 15 days of December of the record, we
 61 used the last 15 days of December and the first 15 days of January, respectively, within the first
 62 (2004) and last (2010) years to complete the 30-day window.

63
 64 The 3-hourly resolution scale factors are then multiplied by *GPP* and *Re*, respectively, for each
 65 3-hourly time step each month:

$$Re_{3hr} = T_{scale} \times Re_{month} \quad (4)$$

$$GPP_{3hr} = I_{scale} \times GPP_{month} \quad (5)$$

66 We modified *Re_{month}* and *GPP_{month}* from Olsen and Randerson (2004) to be given at a 3-hourly
 67 time step, linearly interpolated to 3-hourly time steps based on the present, previous, and
 68 subsequent month, maintaining the original units (g C m⁻² mo⁻¹). *Re_{3hr}* and *GPP_{3hr}* are in units of
 69 g C m⁻² 3hr⁻¹. This modification avoided using the same monthly value for the multiplier for all
 70 3-hourly time steps per month as per Olsen and Randerson (2004), and instead provided a

71 smooth transition from one month to the next. The result of this modification was to eliminate a
72 “ramping” effect whereby values would, for example, increase steadily within a month, then
73 suddenly shift to a new starting point at the beginning of the next month (Figure 1). Note that the
74 original nomenclature of Olsen and Randerson (2004) used $[(2 \times NPP_{month}) - NEP_{month}]$ in
75 place of Re_{month} , and $(2 \times NPP_{month})$ in place of GPP_{month} , where NPP is net primary production
76 (GPP minus autotrophic respiration) and NEP is net ecosystem production (approximately
77 equivalent to the inverse sign of NEE , with caveats (Hayes and Turner, 2012)). The assumption
78 here, therefore, is that $GPP = 2 \times NPP$ and $Re = (2 \times NPP) - NEP$. The Re assumption misses
79 CO_2 emissions other than respiration, e.g., fire, which we correct for at a later step.

80
81 The initial NEE calculation simply subtracts GPP from Re :

$$NEE_{3hr} = Re_{3hr} - GPP_{3hr} \quad (4)$$

82 where NEE_{3hr} is calculated in units of $g\ C\ m^{-2}\ 3hr^{-1}$. However, we applied an additional units
83 conversion for the publicly available data to $kg\ C\ km^{-2}\ s^{-1}$, as these units are more readily
84 ingestible by atmospheric inversion models (Deng et al., 2014).

85
86 Because the downscaling approach uses Re (e.g., autotrophic plus heterotrophic respiration) as
87 the primary CO_2 efflux term, other ecosystem CO_2 loss components, such as fire and other
88 disturbances (Hayes and Turner, 2012), are excluded in the downscale. Hence, the sum of the
89 downscaled 3-hourly NEE fluxes in a given month did not necessarily equal the original monthly
90 NEE flux. So, we included a per-pixel correction whereby we: I) calculated the difference
91 between the sum of the downscaled 3-hourly NEE in a given month and the original monthly
92 NEE ; II) divided that difference by the total 3-hourly time steps in the month, and III) added that
93 difference to each 3-hourly NEE flux. In so doing, the sum of the downscaled 3-hourly NEE
94 fluxes subsequently summed exactly to the original monthly NEE . Nonetheless, this assumption
95 smooths what could otherwise be punctuated fire or disturbance effluxes, so caution should be
96 given when assessing these effluxes at 3-hourly time steps (e.g., relative to observations).

97
98 All input data were given in a spatial resolution of $0.5^\circ \times 0.5^\circ$ (latitude/longitude); hence, we
99 provide the 3-hourly NEE output in $0.5^\circ \times 0.5^\circ$ (Figure 2). We also provide two additional sets of
100 spatially upscaled NEE output in $2.0^\circ \times 2.5^\circ$ and $4.0^\circ \times 5.0^\circ$. These resolutions are used by the
101 atmospheric modeling community, i.e., the GEOS-Chem atmospheric CO_2 transport model in the
102 NASA CMS (Liu et al., 2014). To generate the coarser resolution data we: I) multiplied each
103 pixel value by the land area of that pixel; II) summed the flux from all pixels that represent one
104 pixel in coarser resolution (e.g., 8 x 10 pixels from $0.5^\circ \times 0.5^\circ$ comprise 1 pixel in $4.0^\circ \times 5.0^\circ$);
105 III) calculated the total area covered by the pixels summed in step II; and, IV) divided the value
106 in step II by the value in step III. The regridding preserved the total sum flux of the finer grid
107 cells as well as the total global flux. We provide a file containing the land area contained in each
108 latitudinal band for each of the 3 resolutions (folder name: ‘latitude_area’). We provide two
109 versions of the $2.0^\circ \times 2.5^\circ$ and $4.0^\circ \times 5.0^\circ$ resolution products—one version with consistent
110 global resolution, and another that conforms to the GEOS-Chem setup whereby the northern and
111 southern most latitudinal bands for the $2.0^\circ \times 2.5^\circ$ resolution are $1.0^\circ \times 2.5^\circ$, and for the $4.0^\circ \times$
112 5.0° they are $2.0^\circ \times 5.0^\circ$. The orientation of the global grid in the NetCDF files is transposed (i.e.,
113 $90^\circ S \times 180^\circ W$ at top-left). The time vector represents the mid-point of each 3-hourly period.

115 Processing time in R, un-parallelized, on a standard PC for a single year for the forcing data was
116 as follows:

- 117 • Interpolation of 6-hourly I and T_a to 3-hourly time step: 1 hr per variable
- 118 • 30-day moving window for I : 48 hr
- 119 • 30-day moving window for T_a : 68 hr
- 120 • *Total time to process forcing data for 7 years: $7*(1*2+48+68) = 826$ hr*

121
122 Processing time for the application of the modified Olsen and Randerson (2004) downscaling
123 approach for a single model for a single year was:

- 124 • Monthly interpolation to 3-hourly time steps for GPP : 1 hr
- 125 • Monthly interpolation to 3-hourly time steps for Re : 1 hr
- 126 • GPP and Re downscaling: 2 hr
- 127 • Monthly NEE closure correction: 1 hr
- 128 • NetCDF generation with additional spatial resolutions: 2 hr
- 129 • *Total time to process all 19 products for 7 years: $7*19*(1+1+2+1+2) = 931$ hr*

130
131 The total storage size of the final NetCDF data products for all 19 products (15 models + 4
132 ensemble products) for all 7 years is: 374 GB at $0.5^\circ \times 0.5^\circ$, 38 GB at $2.0^\circ \times 2.5^\circ$, and 10 GB at
133 $4.0^\circ \times 5.0^\circ$.

134
135 We provide the data in NetCDF with a separate file for each day per product at
136 ftp://daac.ornl.gov/data/cms/CMS_NEE_CO2_Fluxes_TBMO/data (Fisher et al., 2016). Each
137 file contains the global gridded data with the eight 3-hourly intervals in the day. Open water
138 pixels are set to 0, as this was desired by the atmospheric modeling community. However, we
139 realize that NEE values can conceivably be 0 (though unlikely as our precision is to 16 decimal
140 places); nonetheless, there are some pixels over land that are calculated as 0, but this is due to
141 missing forcing data (e.g., I in the high latitudes during winter). Our code is set up that we can
142 easily provide a different file output structure and missing value mask by request (contact the
143 corresponding author: jbfisher@jpl.nasa.gov).

144
145 Model output (GPP , Re , and NEE) was from the Multi-scale Synthesis and Terrestrial Model
146 Intercomparison Project (MsTMIP) (Huntzinger et al., 2013; Huntzinger et al., 2016), version 1.
147 15 models were included: 1) BIOME_BGC, 2) CLM, 3) CLM4VIC, 4) CLASS_CTEM, 5)
148 DLEM, 6) GTEC, 7) ISAM, 8) LPJ-wsl, 9) ORCHIDEE, 10) SIB3, 11) SIBCASA, 12) TEM6,
149 13) TRIPLEX-GHG, 14) VEGAS2.1, and 15) VISIT (Table 1). All models were driven by CRU-
150 NCEP meteorological forcing data, hence our use of the same data source for the downscaling
151 approach applied here. We note that there are other meteorological forcing datasets also available
152 at 3-hourly time steps for those interested in applying our downscaling approach with different
153 data (Sheffield et al., 2006; Weedon et al., 2011; Weedon et al., 2014). Although some models
154 are capable of output at sub-monthly time steps, the standard MsTMIP output is at the monthly
155 time step. Additionally, 4 ensemble products were included: 1) un-weighted (naïve) ensemble
156 mean, 2) un-weighted (naïve) ensemble standard deviation, 3) weighted (optimal) ensemble
157 mean, and 4) weighted (optimal) ensemble standard deviation. Weights for model ensemble
158 integration were derived based on model skill in reproducing GPP and biomass (Schwalm et al.,
159 2015). Model output was obtained from:
160 <ftp://nacp.ornl.gov/synthesis/2009/reutlingen/CMS/20141006/>

161
162 To test and confirm that our downscaling approach was applied correctly, we tested our method
163 on a set of ground-truth data of measured *NEE* (and forcing variables) from the FLUXNET
164 database (Baldocchi et al., 2001). We show, for example, a single year for a single site (3-hourly
165 in background with daily-moving window overlaid) (Figure 3) and the scatterplot of calculated
166 versus observed *NEE* values at the 3-hourly time step for that site and year (Figure 4). A full
167 uncertainty analysis of the approach is beyond the scope of this technical note intended to
168 describe the methodological detail of the downscaling.

169 **Acknowledgements**

170 Funding for this work was provided by NASA’s Carbon Monitoring System (CMS) and NASA’s
171 Carbon Cycle Science (CARBON) programs. We thank the MsTMIP modeling teams for
172 providing the model output. Access and information about MsTMIP model output can be found
173 at <http://nacp.ornl.gov/mstmipdata/>, along with model and model team participant information.
174 Funding for the MsTMIP activity was provided through NASA ROSES Grant
175 #NNX10AGO01A. Data management support for preparing, documenting, and distributing
176 MsTMIP model driver and output data was performed by the Modeling and Synthesis Thematic
177 Data Center at Oak Ridge National Laboratory with funding through NASA ROSES Grant
178 #NNH10AN681. We thank Dennis Baldocchi and Siyan Ma for providing the Tonzi Ranch
179 AmeriFlux/FLUXNET data; funding for AmeriFlux data resources and core site data was
180 provided by the U.S. Department of Energy’s Office of Science. The research was carried out at
181 the Jet Propulsion Laboratory, California Institute of Technology, under a contract with the
182 National Aeronautics and Space Administration. Government sponsorship acknowledged.
183 Copyright 2016. All rights reserved.

184 **References**

- 185 Baker, I. T., Prihodko, L., Denning, A. S., Goulden, M., Miller, S., and da Rocha, H. R.:
186 Seasonal drought stress in the Amazon: Reconciling models and observations, *J. Geophys. Res.*,
187 113, G00B01, 2008.
- 188
189 Baldocchi, D., Falge, E., Gu, L. H., Olson, R. J., Hollinger, D., Running, S. W., Anthoni, P. M.,
190 Bernhofer, C., Davis, K., Evans, R., Fuentes, J., Goldstein, A., Katul, G., Law, B. E., Lee, X. H.,
191 Malhi, Y., Meyers, T., Munger, W., Oechel, W., U, K. T. P., Pilegaard, K., Schmid, H. P.,
192 Valentini, R., Verma, S., Vesala, T., Wilson, K., and Wofsy, S. C.: FLUXNET: A new tool to
193 study the temporal and spatial variability of ecosystem-scale carbon dioxide, water vapor, and
194 energy flux densities, *Bulletin of the American Meteorological Society*, 82, 2415-2434, 2001.
- 195
196 Baldocchi, D. and Ma, S.: How will land use affect air temperature in the surface boundary
197 layer? Lessons learned from a comparative study on the energy balance of an oak savanna and
198 annual grassland in California, USA, *Tellus B*, 65, 2013.
- 199
200 Deng, F., Jones, D., Henze, D., Bousserez, N., Bowman, K., Fisher, J., Nassar, R., O'Dell, C.,
201 Wunch, D., and Wennberg, P.: Inferring regional sources and sinks of atmospheric CO₂ from
202 GOSAT XCO₂ data, *Atmospheric Chemistry and Physics*, 14, 3703-3727, 2014.
- 203
204 Fisher, J. B., Huntzinger, D. N., Schwalm, C. R., and Sitch, S.: Modeling the terrestrial biosphere,
205 *Annual Review of Environment and Resources*, 39, 91-123, 2014.
- 206
207 Fisher, J. B., Polhamus, A., Bowman, K. W., Liu, J., Lee, M., Jung, M., Reichstein, M., Collatz,
208 G. J., and Potter, C.: Evaluation of NASA's Carbon Monitoring System Flux Pilot: terrestrial
209 CO₂ fluxes, San Francisco, CA2011.
- 210
211 Fisher, J. B., Sikka, M., Bowman, K. W., Liu, J., Lee, M., Collatz, G. J., Pawson, S., Gunson, M.,
212 CMS Flux Team, TRENDY Modelers, and NACP Regional Synthesis Modelers: The NASA
213 Carbon Monitoring System (CMS) Flux Pilot Project as a means to evaluate global land surface
214 models, American Geophysical Union Fall Meeting, San Francisco, 2012.
- 215
216 Fisher, J. B., Sikka, M., Huntzinger, D. N., Schwalm, C. R., and Liu, J.: CMS: Modeled Net
217 Ecosystem Exchange at 3-hourly Time Steps, 2004-2010. ORNL DAAC, Oak Ridge, Tennessee,
218 USA, 2016.
- 219
220 Hayes, D. and Turner, D.: The need for “apples - to - apples” comparisons of carbon dioxide
221 source and sink estimates, *Eos, Transactions American Geophysical Union*, 93, 404-405, 2012.
- 222
223 Hayes, D. J., McGuire, A. D., Kicklighter, D. W., Gurney, K. R., Burnside, T. J., and Melillo, J.
224 M.: Is the northern high-latitude land-based CO₂ sink weakening?, *Global Biogeochemical*
225 *Cycles*, 25, 2011.
- 226
227 Huang, S., Arain, M. A., Arora, V. K., Yuan, F., Brodeur, J., and Peichl, M.: Analysis of
228 nitrogen controls on carbon and water exchanges in a conifer forest using the CLASS-CTEM N+
229 model, *Ecological Modelling*, 222, 3743-3760, 2011.

230
231 Huntzinger, D., Schwalm, C., Michalak, A., Schaefer, K., King, A., Wei, Y., Jacobson, A., Liu,
232 S., Cook, R., Post, W., Berthier, G., Hayes, D., Huang, M., Ito, A., Lei, H., Lu, C., Mao, J., Peng,
233 C., Peng, S., Poulter, B., Ricciuto, D., Shi, X., Tian, H., Wang, W., Zeng, N., Zhao, F., and Zhu,
234 Q.: The North American Carbon Program Multi-scale synthesis and Terrestrial Model
235 Intercomparison Project–Part 1: Overview and experimental design, *Geoscientific Model*
236 *Development*, 6, 2121-2133, 2013.
237
238 Huntzinger, D. N., Schwalm, C. R., Wei, Y., Cook, R. B., Michalak, A. M., Schaefer, K.,
239 Jacobson, A. R., Arain, M. A., Ciais, P., Fisher, J. B., Hayes, D. J., Huang, M., Huang, S., Ito, A.,
240 Jain, A. K., Lei, H., Lu, C., Maignan, F., Mao, J., Parazoo, N., Peng, C., Peng, S., Poulter, B.,
241 Ricciuto, D. M., Tian, H., Shi, X., Wang, W., Zeng, N., Zhao, F., and Zhu, Q.: NACP MsTMIP:
242 Global 0.5-deg Terrestrial Biosphere Model Outputs (version 1) in Standard Format. DAAC, O.
243 (Ed.), Oak Ridge, Tennessee, USA, 2016.
244
245 Ito, A.: Changing ecophysiological processes and carbon budget in East Asian ecosystems under
246 near-future changes in climate: implications for long-term monitoring from a process-based
247 model, *Journal of plant research*, 123, 577-588, 2010.
248
249 Jain, A. K. and Yang, X.: Modeling the effects of two different land cover change data sets on
250 the carbon stocks of plants and soils in concert with CO₂ and climate change, *Global*
251 *Biogeochem. Cycles*, 19, GB2015, 2005.
252
253 Krinner, G., Viovy, N., de Noblet-DucoudrÈ, N., OgÈe, J., Polcher, J., Friedlingstein, P., Ciais,
254 P., Sitch, S., and Prentice, I. C.: A dynamic global vegetation model for studies of the coupled
255 atmosphere-biosphere system, *Global Biogeochem. Cycles*, 19, GB1015, 2005.
256
257 Li, H., Huang, M., Wigmosta, M. S., Ke, Y., Coleman, A. M., Leung, L. R., Wang, A., and
258 Ricciuto, D. M.: Evaluating runoff simulations from the Community Land Model 4.0 using
259 observations from flux towers and a mountainous watershed, *Journal of Geophysical Research:*
260 *Atmospheres*, 116, 2011.
261
262 Liu, J., Bowman, K. W., Lee, M., Henze, D. K., Bousseres, N., Brix, H., Collatz, G. J.,
263 Menemenlis, D., Ott, L., and Pawson, S.: Carbon monitoring system flux estimation and
264 attribution: impact of ACOS-GOSAT X CO₂ sampling on the inference of terrestrial biospheric
265 sources and sinks, *Tellus B*, 66, 2014.
266
267 Mao, J., Thornton, P. E., Shi, X., Zhao, M., and Post, W. M.: Remote Sensing Evaluation of
268 CLM4 GPP for the Period 2000-09*, *Journal of Climate*, 25, 5327-5342, 2012.
269
270 Olsen, S. C. and Randerson, J. T.: Differences between surface and column atmospheric CO₂
271 and implications for carbon cycle research, *Journal of Geophysical Research: Atmospheres*
272 (1984–2012), 109, 2004.
273

274 Peng, C., Liu, J., Dang, Q., Apps, M. J., and Jiang, H.: TRIPLEX: a generic hybrid model for
275 predicting forest growth and carbon and nitrogen dynamics, *Ecological Modelling*, 153, 109-130,
276 2002.

277

278 Ricciuto, D. M., King, A. W., Dragoni, D., and Post, W. M.: Parameter and prediction
279 uncertainty in an optimized terrestrial carbon cycle model: Effects of constraining variables and
280 data record length, *Journal of Geophysical Research: Biogeosciences (2005–2012)*, 116, 2011.

281

282 Schaefer, K., Collatz, G. J., Tans, P., Denning, A. S., Baker, I., Berry, J., Prihodko, L., Suits, N.,
283 and Philpott, A.: Combined Simple Biosphere/Carnegie-Ames-Stanford Approach terrestrial
284 carbon cycle model, *Journal of Geophysical Research*, 113, G03034, 2008.

285

286 Schwalm, C. R., Huntzinger, D. N., Fisher, J. B., Michalak, A. M., Bowman, K., Ciais, P., Cook,
287 R., El - Masri, B., Hayes, D., and Huang, M.: Toward “optimal” integration of terrestrial
288 biosphere models, *Geophysical Research Letters*, 42, 4418-4428, 2015.

289

290 Sheffield, J., Goteti, G., and Wood, E. F.: Development of a 50-year high-resolution global
291 dataset of meteorological forcings for land surface modeling, *Journal of Climate*, 19, 3088-3111,
292 2006.

293

294 Sitch, S., Smith, B., Prentice, C. I., Arneth, A., Bondeau, A., Cramer, W., Kaplan, J. O., Lucht,
295 W., Sykes, M. T., Thonicke, K., and Venevsky, S.: Evaluation of ecosystem dynamics, plant
296 geography and terrestrial carbon cycling in the LPJ dynamic global vegetation model, *Global
297 Change Biology*, 9, 161-185, 2003.

298

299 Thornton, P. E., Law, B. E., Gholz, H. L., Clark, K. L., Falge, E., Ellsworth, D. S., Goldstein, A.
300 H., Monson, R. K., Hollinger, D., Paw U, J. C., and Sparks, J. P.: Modeling and measuring the
301 effects of disturbance history and climate on carbon and water budgets in evergreen needleleaf
302 forests, *Agricultural and Forest Meteorology*, 113, 185-222, 2002.

303

304 Tian, H., Chen, G., Zhang, C., Liu, M., Sun, G., Chappelka, A., Ren, W., Xu, X., Lu, C., and Pan,
305 S.: Century-scale responses of ecosystem carbon storage and flux to multiple environmental
306 changes in the southern United States, *Ecosystems*, 15, 674-694, 2012.

307

308 Weedon, G., Gomes, S., Viterbo, P., Shuttleworth, W., Blyth, E., Österle, H., Adam, J., Bellouin,
309 N., Boucher, O., and Best, M.: Creation of the WATCH forcing data and its use to assess global
310 and regional reference crop evaporation over land during the twentieth century, *Journal of
311 Hydrometeorology*, 12, 823-848, 2011.

312

313 Weedon, G. P., Balsamo, G., Bellouin, N., Gomes, S., Best, M. J., and Viterbo, P.: The WFDEI
314 meteorological forcing data set: WATCH Forcing Data methodology applied to ERA - Interim
315 reanalysis data, *Water Resources Research*, 50, 7505-7514, 2014.

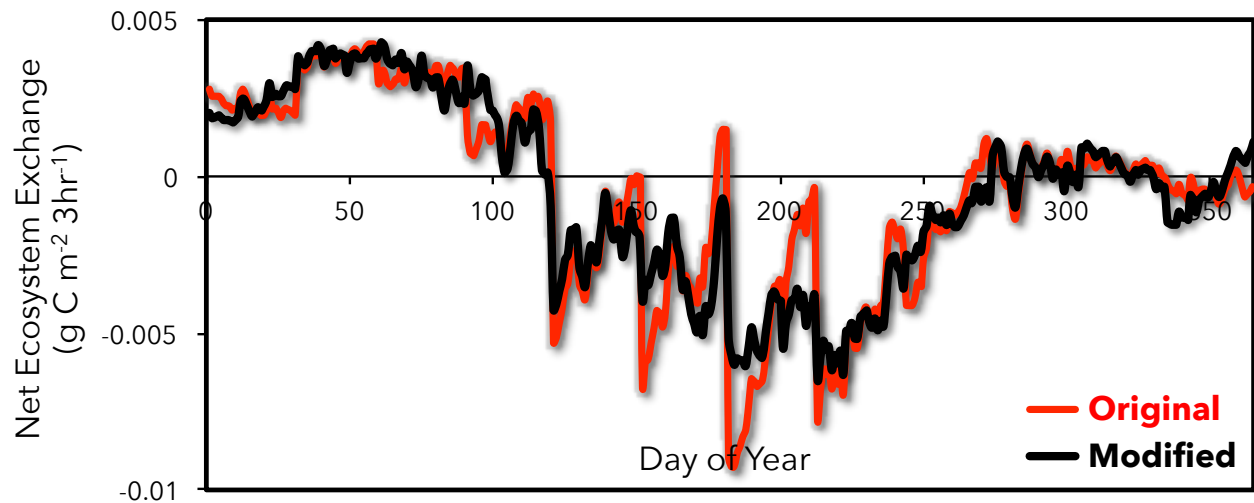
316

317 Wei, Y., Liu, S., Huntzinger, D., Michalak, A., Viovy, N., Post, W., Schwalm, C., Schaefer, K.,
318 Jacobson, A., and Lu, C.: NACP MsTMIP: Global and North American Driver Data for Multi-

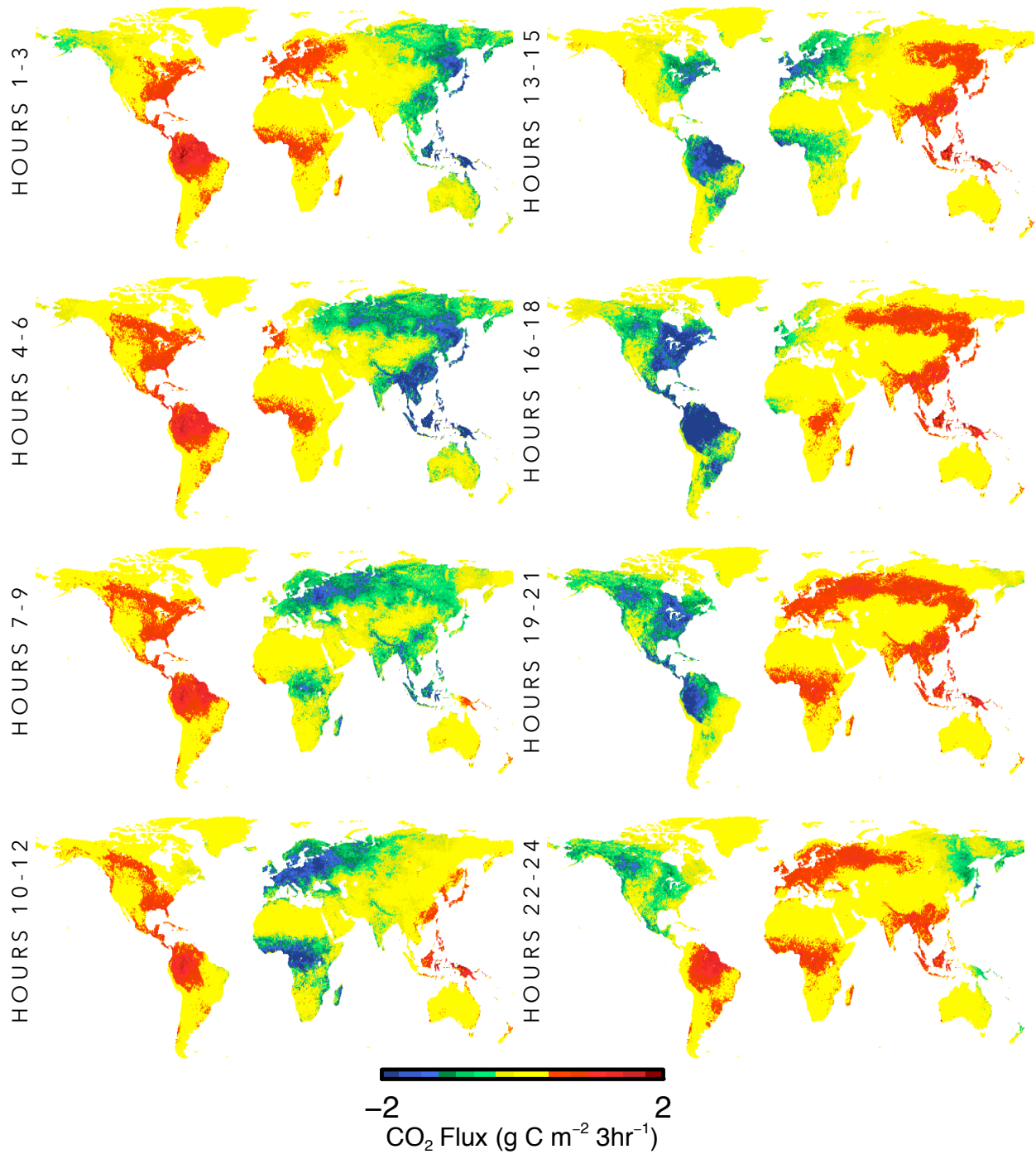
319 Model Intercomparison. Data set. Available on-line [<http://daac.ornl.gov/>] from Oak Ridge
320 National Laboratory Distributed Active Archive Center, Oak Ridge, Tennessee, USA. 2014a.
321
322 Wei, Y., Liu, S., Huntzinger, D., Michalak, A., Viovy, N., Post, W., Schwalm, C., Schaefer, K.,
323 Jacobson, A., and Lu, C.: The North American Carbon Program Multi-scale Synthesis and
324 Terrestrial Model Intercomparison Project–Part 2: Environmental driver data, Geoscientific
325 Model Development, 7, 2875-2893, 2014b.
326
327 Zeng, N., Qian, H., Roedenbeck, C., and Heimann, M.: Impact of 1998-2002 midlatitude drought
328 and warming on terrestrial ecosystem and the global carbon cycle, Geophys. Res. Lett., 32,
329 L22709, 2005.
330
331

Model	Reference
BIOME_BGC	Thornton et al. (2002)
CLM	Mao et al. (2012)
CLM4VIC	Li et al. (2011)
CLASS_CTEM	Huang et al. (2011)
DLEM	Tian et al. (2012)
GTEC	Ricciuto et al. (2011)
ISAM	Jain and Yang (2005)
LPJ-wsl	Sitch et al. (2003)
ORCHIDEE	Krinner et al. (2005)
SIB3	Baker et al. (2008)
SIBCASA	Schaefer et al. (2008)
TEM6	Hayes et al. (2011)
TRIPLEX-GHG	Peng et al. (2002)
VEGAS2.1	Zeng et al. (2005)
VISIT	Ito (2010)

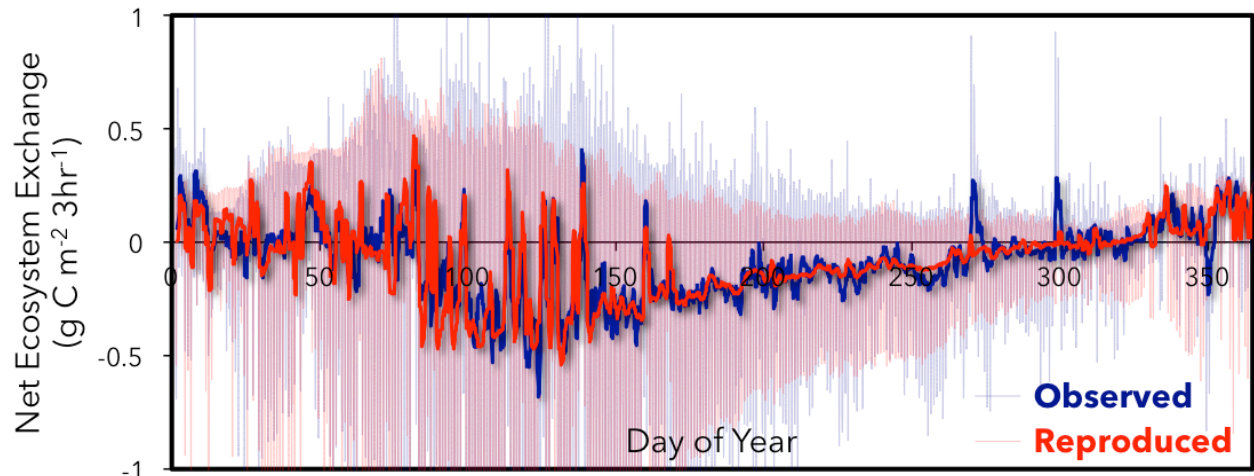
332 Table 1. Global terrestrial biosphere models from the Multi-scale Synthesis and Terrestrial
333 Model Intercomparison Project (MsTMIP) downscaled in this activity.



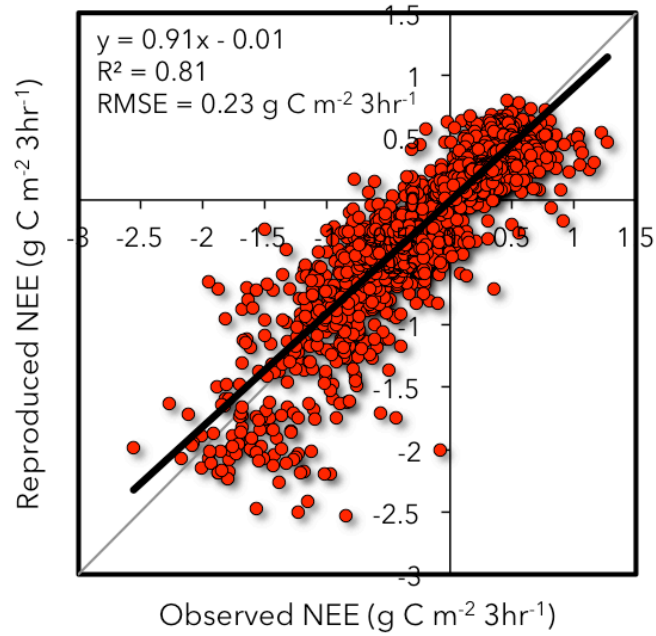
334
 335 Figure 1. The original downscaling approach of Olsen and Randerson (2004) used monthly fixed
 336 values, which led to a “stair-stepping” behavior between months (red). This was eliminated by
 337 using a 30-day moving window and interpolating monthly input values to 3-hourly time steps
 338 (black). Example shown for LPJ model global mean year 2005.



339 Figure 2. Vegetation productivity (e.g., blues/greens) follows the course of the sun for a single
 340 day of net ecosystem exchange (NEE or net CO₂ flux; g C m⁻² 3hr⁻¹) for each 3-hourly period.
 341 Shown here, for example, is July 1, 2007 for the weighted ensemble mean product.



342
343 Figure 3. The observed net ecosystem exchange (NEE) (blue) and reproduced NEE (red) shown
344 at the 3-hourly time step with daily moving window overlaid for a single year from the Tonzi
345 Ranch AmeriFlux/FLUXNET site (Baldocchi and Ma, 2013).



346
347 Figure 4. Observed versus reproduced net ecosystem exchange (NEE) at the 3-hourly time step
348 for a single year at the Tonzi Ranch AmeriFlux/FLUXNET site (Baldocchi and Ma, 2013).